First observation of feshbach resonances at very low magnetic field in a 133Cs fountain

Document status and date:
Published: 01/07/2004

Document Version:
Accepted manuscript including changes made at the peer-review stage

Please check the document version of this publication:

• A submitted manuscript is the version of the article upon submission and before peer-review. There can be important differences between the submitted version and the official published version of record. People interested in the research are advised to contact the author for the final version of the publication, or visit the DOI to the publisher's website.
• The final author version and the galley proof are versions of the publication after peer review.
• The final published version features the final layout of the paper including the volume, issue and page numbers.

Link to publication

Download date: 08. Jul. 2024

FIRST OBSERVATION OF FESHBACH RESONANCES AT VERY LOW MAGNETIC FIELD IN A ^{133}CS FOUNTAIN.

H. Marion,[*] S. Bize, L. Cacciapuoti,[†] D. Chambon, F. Pereira dos Santos, G. Santarelli, P. Wolf,[‡] and A. Clairon

BNM-SYRTE, Observatoire de Paris, 61 Avenue de l'Observatoire, 75014 Paris, France.

A. Luiten and M. Tobar

The University of Western Australia, School of Physics, 35 Stirling Hwy, Crawley, Western Australia.

S. Kokkelmans[§] and C. Salomon

Laboratoire Kastler Brossel, ENS, 24 rue Lhomond, 75005 Paris, France.

For a long time, one of the main limitations of cesium atomic fountains has been the cold collision frequency shift [2, 7, 10, 11, 26]. By using a method based on a transfer of population by adiabatic passage (AP) [12, 17, 19] allowing to prepare cold atomic samples with a well defined ratio of atomic density as well as atom number we have a better measurement of this effect. By improving the method we found out some unexpected properties of cold collisions, confirming that ^{133}Cs is a rich atom to study cold collisions. Those results lead to fine comparisons with cold collision theory and may constraint some parameters of cesium.

Frequency standards are used in many industrial (Global Positioning System, navigation) and scientific pursues (fundamental physic tests [5, 15, 16]). Primary standards are today based on cesium and are contributing to the realization of the second. The most accurate are using cold atoms to allow long interaction time. In cold atomic gases collisions play an important role by shifting the clock frequency. Thus, it is crucial to control and to study accurately cold collisions for clock uncertainty budget. Nevertheless, there is a tradeoff between the clock stability and its accuracy. In this paper we will describe improvement of the a technic based on fast AP that allows to reconcile those two goals. For high density atomic sample, such as in Bose-Einstein condensates (BEC) [1], manifestations of collision such as molecular Feshbach resonances [8, 24] are observed. We found out, in our fountain, such phenomenon at very low magnetic field and density. Theoretical tools will be remind and a numerical simulation of some of our data will be presented.

THE DOUBLE FOUNTAIN: RECENT IMPROVEMENTS AND PERFORMANCES.

Atom loading improvement.

At Paris observatory, there is a set of three atomic fountains, using cesium. In particular, our one is a double fountain [4, 16, 26] able to work alternatively with rubidium and cesium. In the last year, on the cesium part, we improved the loading rate by supplementing a transverse collimation of the atomic beam in addition to the present chirp cooling (see FIG. 1). It consists in a 2D optical molasses with two laser beams, recycling the light in a "zigzag" way [20, 22]. This allows us to cool 10^9 atoms in 200 ms in an optical molasses. The 2D molasses increase the loading rate by a factor of ~ 10. Regular parameters of the double fountain are a magnetic field in the interrogation zone of 2 mG, a loading duration of $\sim$ 200 ms that allows to load 10^9 atoms within a fountain cycle of ~ 1.2 s. The launch velocity is ~ 4 m.s^{-1} that imply a launch height of ~ 0.8 m.

Frequency stability.

A sapphire cryogenic oscillator (SCO) [13] from the University of Western Australia is now used as a filter for one of our H-maser. The SCO is an experiment by itself [25], but is very reliable and can be used routinely to drive the fountain. The SCO is weakly phase-locked on the H-maser with a time constant of about an hour. Therefore, the resulting signal reflects the good short term stability of the SCO while in long time scales it reproduce the characteristics of the H-maser. The SCO delivers a signal of about 12 GHz.

At BNM-SYRTE most of the microwave synthesizer use a 100 MHz signal to generate the 9.2 GHz necessary to interrogate the atoms. Therefore, a down-converter has been developed to transform the SCO signal into a 100 MHz one. An evaluation has shown that the foun-
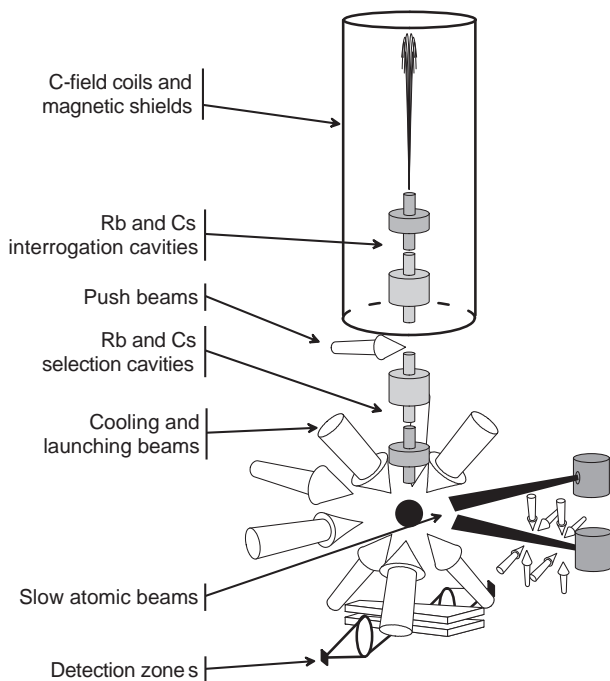
FIG. 1: Schematic of the double fountain both base on ^{87}Rb and ^{133}Cs, so that there is two pairs of cavity finely tuned on hyperfine atomic frequency of corresponding atoms and two ovens. On the cesium part, a transversal collimation of the atomic beam has been improved in addition of the present chirp cooling. This consists in a 2D recycling light, pair of laser beam, used in a "zigzag" way. This allows to load around 10^9 atoms in 200 ms in an optical molasses.

tain was limited by the phase noise of the microwave setup. Henceforth, a new microwave synthesizer [6] able to down-convert directly the 12 GHz to 9.2 GHz has been built in order to minimize the phase noise. It achieves a frequency stability of $\sim 3\ 10^{-15}$ at 1s. In order to take benefits of its excellent short term stability ($\sim 5\ 10^{-16}$ at 1s) a large number of trapped atoms is required [21]. With $\sim 10^7$ detected atoms we were able to reach $1.6\ 10^{-14}$ at 1 s, the best frequency stability for a primary standard to date. With this performances a resolution of 10^{-16} is achievable in 6 hours.

FIG. 2 shows the Allan deviation of the fountain driven by the SCO. This is a differential measurement [23], this means that a full atom number configuration (■) is alternated with a half atom number configuration (●) each 60 fountain cycles. The (■) represents the fractional frequency deviation of the corrections applied to the interrogating microwave generated with the SCO signal to stay at resonance with the atoms. This is performed with the maximum atom number (N_{at}) which allows the $1.6\ 10^{-14}$ at 1s stability. On short term (10 s to 100 s) the allan variance is dominated by the Cs fountain noise. After 200 s, the drift of the SCO is observed. The Allan deviation of the frequency difference between low ($N_{at}/2$) and high(N_{at}) density (▲) averages as white frequency noise
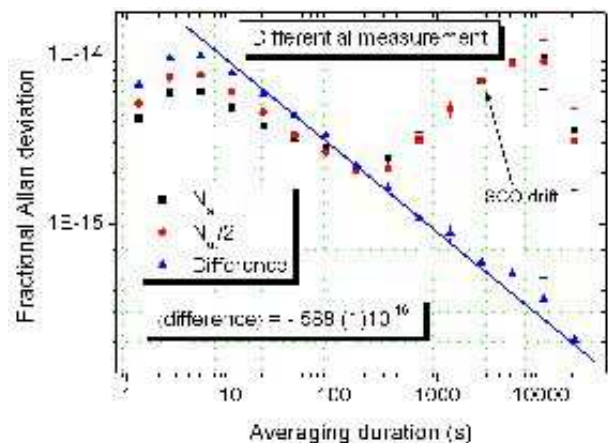

FIG. 2: Shows the Allan deviation of the fountain driven by the SCO. This is a differential measurement of the collisional shift, this means that a full atom number configuration (■) is alternated with a half atom number configuration (●) each 60 fountain cycles. The (■) represents the fractional frequency deviation of the corrections applied to the interrogating microwave generated with the SCO signal to stay at resonance with the atoms. This is performed with the maximum atom number which allows the $1.6\ 10^{-14}$ at 1 s stability. The Allan deviation of the difference (▲) averages well for all times and has also a good stability. This leads to a good statistical evaluation of the mean difference in a very reasonable time.

for all times and reaches $\sim 2\ 10^{-16}$ for a 20000 s measurement. This leads to a good statistical evaluation of the mean difference in very reasonable time. The SCO drift is efficiently rejected and atom number dependent effects (i.e. cavity pulling [3] and collisional shift) are measured with a statistical uncertainty of 10^{-16} in one day. This behavior indicates that determination of the collisional frequency shift is only limited by the frequency stability of the fountain.

ACCURATE CONTROL OF COLD COLLISION FREQUENCY SHIFT.

In previous work [16, 19], we demonstrated the possibility to control and evaluate the cold collision shift at the percent level by using the adiabatic passage method. Cold collisions represent the main systematic effect that shifts the frequency and restricts the accuracy in cesium fountains. At that time, our collisional shift for full density, was around 10^{-14}. Therefore, the corresponding uncertainty was near 10^{-16}.

Adiabatic passage performances.

To achieve a stability around $\sim 2\ 10^{-14}$ at 1 s it is necessary to load a high number of atoms. For example the collisional shift corresponding to N_{at} of the (■) curve
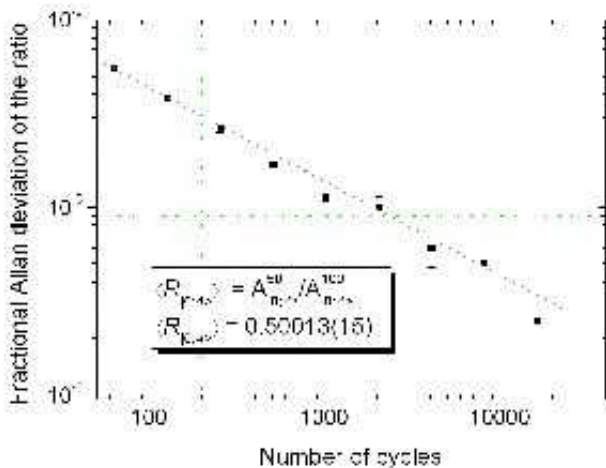
FIG. 3: Allan deviation of the ratio of atom numbers in the $|4;0\rangle$ obtained by alternating each 60 fountain cycle a full atom number configuration over half atom number configuration on the $|4;0\rangle$ state as a function of cycle number. The Allan deviation of the ratio averages as white noise and reaches $\sim 10^{-3}$ resolution after 1 hour. It leads to evaluate AP at the 10^{-3} level.

implies a frequency shift of about $\sim 1.2\ 10^{-13}$. Thus, an AP at the percent level is no longer enough to stay at the 10^{-16} level of uncertainty on this effect. To perform AP the amplitude of the microwave into the selection cavity has to be modulated and its frequency has to be swept. It is critical that the synthesizer used to chirp the selection microwave stops the frequency sweep at resonance for the half AP. Our model (Marconi 2030) was not accurate enough and failed to be reproducible. It has been replaced by a DDS more easily frequency controllable. According to [16, 19], one observable for AP evaluation is the ratio of atom number at full and half density. Each measurement is daily analyzed using this criterion to verify that the AP method is properly working.

FIG. 3 shows the Allan deviation of the ratio of atom numbers in the $|4;0\rangle$ obtained by alternating each 60 fountain cycle a full atom number configuration over half atom number configuration as a function of cycle number. The Allan deviation of the ratio averages as white noise and reaches $\sim 10^{-3}$ resolution after 1 hour. It leads to evaluate AP at the 10^{-3} level such as:

$$\frac{A^{(50)}_{|4;0\rangle}}{A^{(100)}_{|4;0\rangle}} = \frac{\tilde{n}^{(50)}_{|4;0\rangle}}{\tilde{n}^{(100)}_{|4;0\rangle}} = \frac{1}{2} \times (1 + 1\ 10^{-3})$$

Where $\tilde{n}^{(100)}_{|4;0\rangle}$ ($\tilde{n}^{(50)}_{|4;0\rangle}$) is the density of the $|4;0\rangle$ atoms for full atom number (half atom number) and $A^{(100)}_{|4;0\rangle}$ ($A^{(50)}_{|4;0\rangle}$) is the detected atom number on the $|4;0\rangle$ for full atom number (half atom number).

The deviation measured at the 10^{-3} level could be induced by a non linearity in the detection. This will be investigated in a future work.

Similarly, we also check routinely the same ratio on the F = 3 level. Here, we find a larger deviation:

$$\frac{A^{(50)}_{|3;0\rangle}}{A^{(100)}_{|3;0\rangle}} = \frac{\tilde{n}^{(50)}_{|3;0\rangle}}{\tilde{n}^{(100)}_{|3;0\rangle}} = \frac{1}{2} \times (1 + 3\ 10^{-3})$$

The departure of $3\ 10^{-3}$ from the $1/2$ ratio is due to residual populations in the $|3;m_{\mathrm{F}}\rangle$ states. A fraction of the atoms is coming from the push beam (see FIG. 1, i.e. a laser beam that finalize to the selection process) which is de-pumping atoms from the $|4;m_{\mathrm{F}}\rangle$ states to the $|3;m_{\mathrm{F}}\rangle$ states. The remanning fraction seem to be launched in the F = 3 state. Attempts to remove these atoms with extra repumper beams where partially unsuccessful. At this point, there is nothing much to do to prevent it but to look at the contribution of those spurious atoms on the clock shift.

Towards an adiabatic passage at the 10^{-3} level.

An accurate control of the collisional shift is possible only if the contribution of the 0.3 % atoms populating states different from the clock states is correctly evaluated. To measure this, we intentionally populated the atomic cloud using AP with $|3;m_{\mathrm{F}} \neq 0\rangle$ states in addition of the $|3;0\rangle$ clock state. An additional microwave synthesizer tuned on a $|4;m_{\mathrm{F}} \neq 0\rangle \to |3;m_{\mathrm{F}} \neq 0\rangle$ transition is combined in the selection cavity with the regular selection synthesizer. A magnetic field is applied during the selection by AP in order to prevent parasitic excitations between zeeman sub-levels. To select, for example $m_{\mathrm{F}} = 1$ state, one has to detune from resonance the extra synthesizer of the corresponding first order Zeeman shift value.

The measurement method alternate three different fountain configurations. The first one is a full AP selection of the $|3;0\rangle$ state, the second is a half AP selection of the $|3;0\rangle$ state. The first configurations give the collisional shift due to the clock states. The third one is a full AP selection of the $|3;0\rangle$ state plus full AP selection of one of the $|3;m_{\mathrm{F}} \neq 0\rangle$ states. The last configuration combined with the two others lead to a measurement the collisional shift due to the extra population. The respective frequency shifts are:

$$\Delta\nu_1/2\pi = \tilde{n}_{00}K_{00}$$
$$\Delta\nu_2/2\pi = \frac{\tilde{n}_{00}}{2}K_{00}$$
$$\Delta\nu_3/2\pi = \tilde{n}_{00}K_{00} + \tilde{n}_{m_{\mathrm{F}}m_{\mathrm{F}}}K_{m_{\mathrm{F}}m_{\mathrm{F}}}$$

Where $\tilde{n}_{00}$ ($\tilde{n}_{m_{\mathrm{F}}m_{\mathrm{F}}}$) represents the atom density of the clock states (m_{F} states), and K_{00} ($K_{m_{\mathrm{F}}m_{\mathrm{F}}}$) is the cold
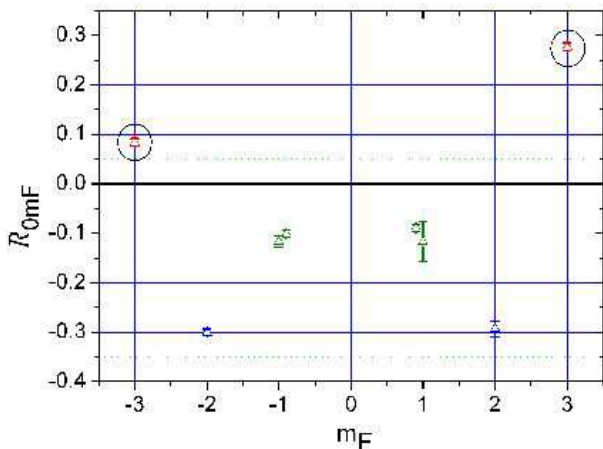
FIG. 4: displays R_{0m_F} as a function of the m_F value for regular clock conditions. The contribution to the cold collision shift of the $|m_F| = 1$; 2 are negative and equal for the same absolute values. At most the contribution of spurious $|3; m_F \neq 0\rangle$ is 1/3 of the contribution of clock states. The contribution of the $|m_F| = 3$ is different.

FIG. 5: Ratio R_{01} as a function of the magnetic field. It represents a Feshbach resonance for $|m_F| = 1$.

collisional shift coefficient resulting of the extrapolated to zero density for the clock states (m_F states).

Under regular operating conditions, we evaluate the contribution to the clock shift due to the collisional shift of the extra $|3; m_F \neq 0\rangle$ atoms per detected atom ($\nu_{m_F m_F}$ in Hz.(detected atoms)$^{-1}$) normalized to the collisional shift of the clock states $|3; 0\rangle$ atoms per detected atoms (ν_{00}) as a function of the m_F value. This ratio (R_{0m_F}) can be expressed as:

$$\begin{aligned} R_{0m_F} &= \frac{\nu_{m_F m_F}}{\nu_{00}} \\ &= \frac{\Delta\nu_3 - \Delta\nu_1}{2(\Delta\nu_1 - \Delta\nu_2)} \frac{N_{00}}{N_{m_F m_F}} \end{aligned}$$

Were N_{00} ($N_{m_F m_F}$) is the detected atoms number for the clock states (m_F state) and can be expressed as $N_{00} = A_{|3;0\rangle} + A_{|4;0\rangle}$. A verification that ν_{00} is field independent has been performed so that it could be used as a reference. It is important to ensure that the density is the same whatever the could is made of. Thus a verification that the spatial distribution of the different Zeeman sub-levels is homogenous into the cloud has been performed. By selecting one m_F at the time and pulsing the Ramsey cavity with different durations, we access at different cloud slice. It shows that the peak density are equal to less than 7 %.

FIG. 4 displays R_{0m_F} as a function of the m_F value for regular conditions ($B \simeq 2\ mG$). The contribution to the cold collision shift of the $|m_F| = 1$; 2 are negative and equal for the same absolute values. At most the contribution of spurious $|3; m_F \neq 0\rangle$ is 1/3 of the contribution of clock states. Thus, the collisional shift is controlled at the 10^{-3} level. Surprisingly the contribution of the
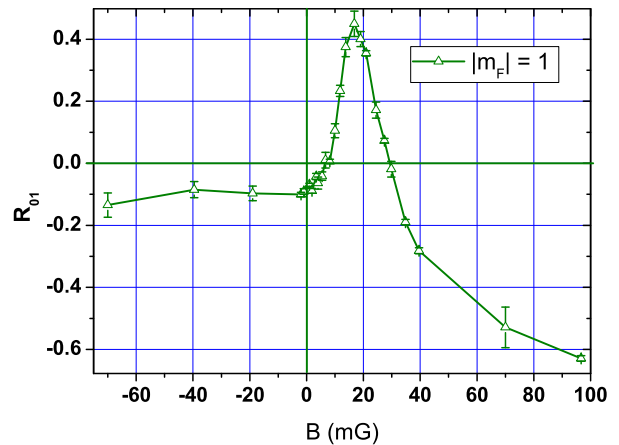
$|m_F| = 3$ is different, which was unpredicted at such low magnetic field. This observation is a clear indication of the presence of Feshbach resonances.

FESHBACH RESONANCES.

Experimental results.

We thus looked for the ratio (R_{0m_F}), for each absolute value of the m_F as a function of magnetic field. We found out three Feshbach resonances (FIGs. 5, 6 and 7) deeply field dependent. It gives a direct access to the amplitude and the width of each resonance. The field is very well controlled so that there is no way that error bars could mix up the shapes. For some values of the magnetic field the frequency shift due to $|3; m_F\rangle \neq 0$ population can be as large as the standard clock shift. Let's remind that our regular magnetic field is 2 mG. One has to be very cautious by choosing a value of magnetic field in an experiment using cold ^{133}Cs. The $|m_F| = 2$ resonance is obviously a multiple resonance, but the $|m_F| = 1$ and specially $|m_F| = 3$ look to be more simple. Assuming that $|m_F| = 3$ resonance is a simple resonance we try to understand the line shape with a simple model.

Theoretical approach: model for S-matrix.

In order to describe the measured resonances, we need to account for the inelastic collision processes. Feshbach resonances in cold atomic systems are usually considered only in the context of elastic scattering, with one open channel only [14, 18]. In such a situation, only an elastic resonance width Γ_e is involved, and the incoming channel for the atoms is simultaneously the exit channel. Here we consider a situation with more than one open chan-
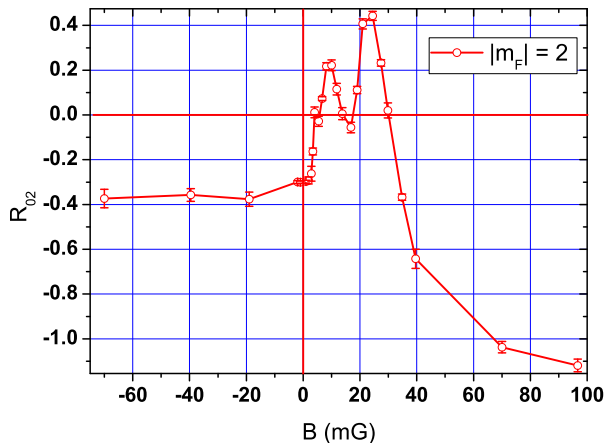
FIG. 6: Ratio R_{02} as a function of the magnetic field. It represents a Feshbach resonance for $|m_\mathrm{F}| = 2$. This is obviously a multiple resonance.
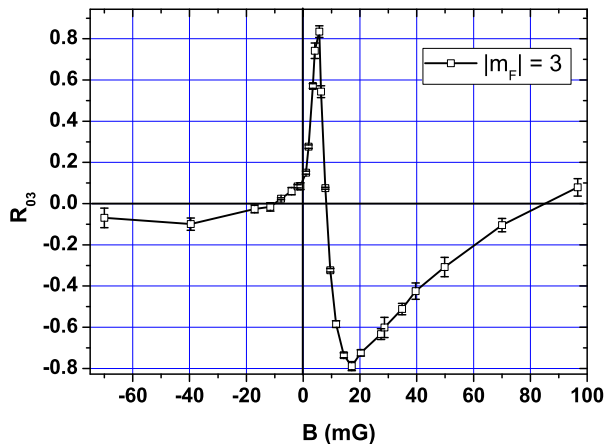

FIG. 7: Ratio R_{03} as a function of the magnetic field. It represents a Feshbach resonance for $|m_\mathrm{F}| = 3$. This resonance has a more simple shape. Assuming that it is a simple resonance we gone to simulate the scattering process.

nel. Atoms which exit in a different channel than the incoming channel will gain additional kinetic energy, and are considered as lost. This decay process can be mediated via the molecular Feshbach state, and gives rise to an additional energy scale, the inelastic resonance width Γ_i [9].

The S-matrix for such an inelastic resonance can be written as

$$S(k) = S^{bg}(k)\left(1 - \frac{i\Gamma_e(k)}{E - \nu + \frac{1}{2}i\Gamma_e(k) + \frac{1}{2}i\Gamma_i(k)}\right) \quad (1)$$

with $E = \hbar^2 k^2/m$ the relative kinetic energy between the colliding atoms, $\nu = \Delta\mu(B - B_0)$ the detuning, and $S^{bg}(k) = \exp(-2ika_{bg})$ the background (or direct) part of the S-matrix. Here B_0 is the magnetic field value of resonance, and $\Delta\mu$ the difference between the magnetic

moments of the two particles in the incoming channel and the molecular Feshbach state. The background scattering length $a_{bg} = a_{bg}^r + ia_{bg}^i$ contains not only a real part a_{bg}^r, but also an imaginary part a_{bg}^i since there is also a direct contribution to the inelastic decay.

The energy widths are in principle a function of the relative wavenumber k, since they depend on the overlap between the molecular wavefunction corresponding to the Feshbach state, and the wavefunction in the corresponding open channel. In case of the elastic energy width, the energy dependence of the incoming channel gives rise to linear dependence in wavenumber, i.e. $\Gamma_e = c_e k$ with c_e a constant [18]. For the inelastic energy width, however, the energy dependence of the corresponding open channels can be safely neglected over the energy range of interest. Therefore Γ_i can be taken energy-independent.

Monte Carlo model.

The frequency shift of the clock transition due to the $|3; m_F \neq 0\rangle$ state population is given by Eq. (2):

$$\frac{\delta\omega_{\beta\alpha}}{2\pi} = \frac{\hbar\rho_{\gamma\gamma}}{mk}Im\left\{S_{\alpha\gamma}(k)S_{\beta\gamma}^\dagger(k) - 1\right\} \quad (2)$$

where α and β refer to the $|3; 0\rangle$ and $|4; 0\rangle$ clock states respectively. $\rho_{\gamma\gamma}$ is the atomic density of the $|3; m_\mathrm{F} \neq 0\rangle$ state (denoted as γ). To be consistent with our initial intent to analyze the $|m_\mathrm{F}| = 3$ data as a single Feshbach resonance, we will assume that a resonance occurs for only one of the two entrance channels ($\alpha\gamma$ and $\beta\gamma$). The other entrance channel contribute only with a constant background part, independent on the magnetic field. This factor can be formally accounted for in the background term of the channel where the resonance occurs. Therefore, we are assuming that $S_{\alpha\gamma} = 1$ (resp. $S_{\beta\gamma} = 1$) while $S_{\beta\gamma}(k)$ (resp. $S_{\alpha\gamma}(k)$) follows Eq. (1).

Eq. (2) clearly shows that the clock shift depends on the wavenumber k. The total clock shift is obtained by suitably averaging Eq. (2) over the duration of the interrogation, taking into account the atomic cloud space and velocity distribution. This is done using a Monte Carlo simulation where the atomic trajectories are randomly sampled according to the space and velocity distributions as measured in the experiment (with CCD imaging and analysis of time of flight signals). The simulation accounts for the distribution of collisional energy, for the time varying (decreasing) atomic density, for the non-uniform response of the final transition probability to a time varying perturbation (sensitivity function), for the truncation of the atomic cloud crossing the microwave resonator.

FIGs. 8 and 9 represent examples of calculated line shape of the Feshbach resonance for various parameters. For all cases, we take $a_{bg} = 0$, $B_0 = 0$ and $\Delta\mu = 2\mu_B$. Also, we assume that the resonance occurs on the $\beta\gamma$
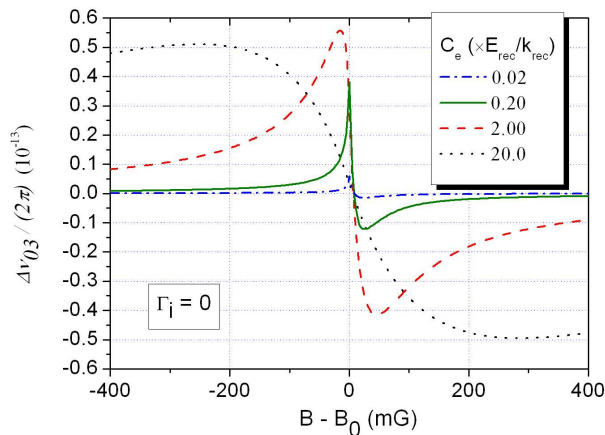
FIG. 8: For $\Gamma_i = 0$. For large values of C_e, the shape and the ("natural") width of the resonance is determined by C_e. The resonance has a symmetrical dispersive shape. For small values of C_e, the shape and the width of the resonance is determined by the collision energy distribution. The line shape shows a strong asymmetry. The calculation clearly indicates that the top of the sharp feature corresponds to the magnetic field that meets the resonant condition.
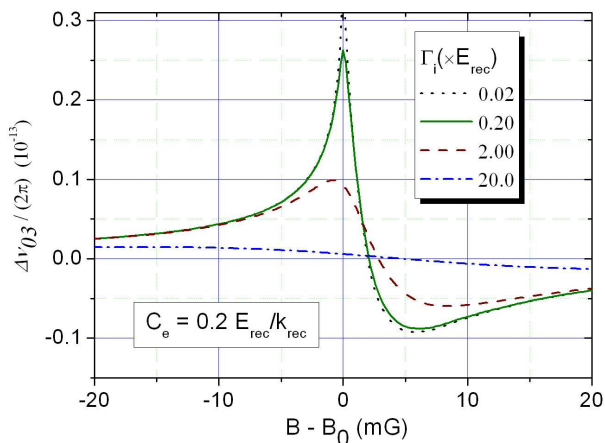

FIG. 9: illustrates the effect of parameter Γ_i. C_e is kept constant. The resonance shape is computed for different Γ_i amplitudes. The comparison with the measured line shape clearly indicates that the observed resonance are not strongly affected by the inelastic processes. The calculation shows that the sign of the clock shift is inverted when the resonance occur on the $\alpha\gamma$ channel.

channel. The initial distribution is gaussian with $\sigma = 3.5$ mm. The velocity distribution is $\propto (1+v^2/v_c^2)^{-b}$ with $v_c = 10$ mm.s^{-1} and $b = 2.1$. The vertical axis represents the fractional frequency shift due to the γ ($|3; m_F\rangle$) state for 10^8 atoms launched in this state. This corresponds to a typical effective atomic density of $2.2 \ 10^7$ cm^{-3}. In FIG. 8, $\Gamma_i = 0$. C_e is equal to $0.2 \times E_{rec}/k_{rec}$, $2 \times E_{rec}/k_{rec}$, $20 \times E_{rec}/k_{rec}$ and $200 \times E_{rec}/k_{rec}$ where $E_{rec} = \hbar^2 k_{rec}^2/2m$ and $k_{rec} = 2\pi/\lambda$, $\lambda = 852$ nm. For large values of C_e, the shape and the ("natural") width of
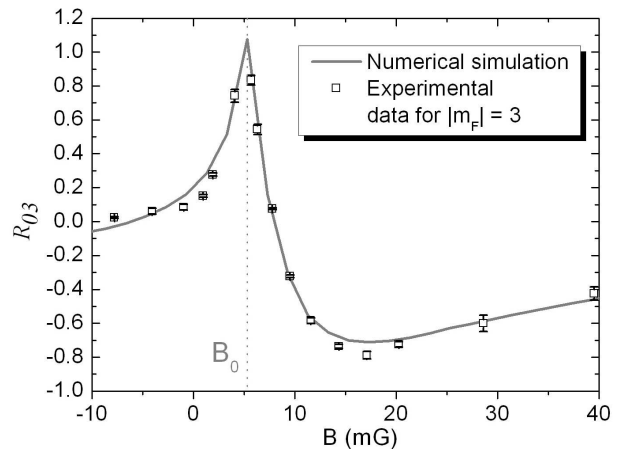

FIG. 10: The $|m_F| = 3$ data are in good agreement with a resonance dominated by the collision energy. The Monte Carlo model fits well the point and indicates the resonant field.

the resonance is determined by C_e. The resonance has a symmetrical dispersive shape. For small values of C_e, the shape and the width of the resonance is determined by the collision energy distribution. The line shape shows a strong asymmetry. The calculation clearly indicates that the top of the sharp feature corresponds to the magnetic field that meets the resonant condition (vanishing difference between the molecular bound state energy and the dissociation threshold). Similarly, FIG. 9 illustrates the effect of parameter Γ_i. C_e is kept constant and equal to $0.2 \times E_{rec}/k_{rec}$. The resonance shape is computed for Γ_i equal to $0.02 \times E_{rec}$, $0.2 \times E_{rec}$, $2 \times E_{rec}$ and $20 \times E_{rec}$. The comparison with the measured line shape clearly indicates that the observed resonance are not strongly affected by the inelastic processes. Finally, the calculation (as well as direct consideration of Eq. (1) shows that the sign of the clock shift is inverted when the resonance occur on the $\alpha\gamma$ channel.

The measured $|m_F| = 3$ resonance is fitted (see FIG. 10) using the above model leaving B_0, $\Delta\mu$, C_e, Γ_i, a_{bg} as free parameters. The model also includes the possibility of a slow variation of the background scattering length with the magnetic field through the addition of a linear and quadratic term as a function of the magnetic field. We checked that the following analysis is not significantly affected by this additional term. Finally, the model includes a scale factor for the atomic density. Similarly, the inclusion of this scale factor has no influence on the following analysis.

The simple consideration of the sign of the data indicates that the resonance occurs in the $\beta\gamma$ channel involving the upper clock state $|4; 0\rangle$ and the $|3; 3\rangle$ state. FIG. 10 shows the optimized fit to the data. The qualitative agreement with the model is quite satisfactory. For $\Delta\mu$, C_e and Γ_i, the analysis does not lead to precise

value, due to the sensitivity of these parameters to the atomic cloud space and velocity distribution. We find $\Delta\mu \simeq 1.5\mu_B$, $C_e \sim 0.2 E_{rec}/k_{rec}$ and $\Gamma_i \lesssim 0.2 \times E_{rec}$. Conversely, B_0 is tightly constrained and well decorrelated from the other parameters. Although an uncertainty on B_0 cannot be easily extracted from our (nonlinear) fitting procedure, we can safely state that B_0 is constrained to within 1 mG (to be understood as a 1σ error bar). We find $B_0 = 5 \pm 1$ mG, this corresponds to 500 ± 100 nK, expressed in temperature scale. This is, to our knowledge, the lower molecular bound state energy ever involved in Feshbach resonances (*i.e.* around 10 kHz from the continuum).

CONCLUSION.

To sum-up, our primary goal is achieved, the collisional shift is controlled at the 10^{-3} of its value. A calibration of Zeeman sub-states contribution to the clock shift as a function of the field has been performed and teaches us magnetic field values to avoid. Under regular clock conditions an upper limit for their contribution shows an upper limit compatible with AP at the 10^{-3} level. This makes reachable the goal of primary standards at the 10^{-16} uncertainty level. Feshbach resonances have been observed for the first time at very low magnetic field and with a very good resolution. A Monte Carlo simulation has been performed and could fit properly some of experimental data. This constrains some parameters of the theory of collisions.

---

[*] Present address: Institut d'Optique Thorique et Appliquée. Bat 503, Centre Scientifique d'Orsay, 91403, Orsay, France

[†] Present address: Dipartimento di Fisica, Universita degli studi di Fireze, via Sansone 50019 Steso Firentino (FI), Italy

[‡] Present address: Bureau International des Poids et Mesures, Pavillon de Breteuil, 92312, Sèvres cedex, France

[§] Present address: Eindhoven University of Technology, P.O. Box 513, 5600 MB Eindhoven, The Netherlands

[1] M.H. Anderson *et al.*, Science **269**, 198 (1995).
[2] M. Bijlsma *et al.*, Phys. Rev. A **49**, R4285 (1994).
[3] S. Bize *et al.*, IEEE Trans. on Instr. and Meas. **50**, 503 (2001)
[4] S. Bize *et al.*, in *Proc. of the 6th Symposium on Frequency Standards and Metrology* (World Scientific, Singapore, 2001), p 53.
[5] S. Bize *et al.*, Phys. Rev. Lett. **90**, 150802 (2003).
[6] D. Chambon *et al.*, Proceeding EFTF 2004.
[7] C. Chin *et al.*, Phys. Rev. A **63**, 033401 (2001).
[8] H. Feshbach, Ann. of Phys. (N.Y.) **5**, 357 (1958); **19**, 287 (1962).
[9] H. Feshbach, *Theoretical Nuclear Physics* (John Wiley and Sons, New York, 1992).
[10] S. Ghezali *et al.*, Europhys. Lett. **36**, 25 (1996).
[11] K. Gibble and S. Chu, Phys. Rev. Lett. **70**, 1771 (1993).
[12] M.M.T. Loy, Phys. Rev. Lett. **32**, 814 (1974).
[13] A. Luiten *et al.*, IEEE Trans. on Instr. and Meas. **44**, 132 (1995).
[14] B. Marcelis, E.G.M. van Kempen, B.J. Verhaar, and S.J.J.M.F. Kokkelmans, cond-mat/0402278.
[15] H. Marion *et al.*, Phys. Rev. Lett. **90**, 150801 (2003).
[16] H. Marion, *Controle des collisions froides du 133Cs, test de la variation de la constante de structure fine laide dune fontaine atomique double rubidium - cesium*, PhD Thesis, Universite Paris VI, (2005).
[17] A. Messiah, Quantum Mechanics, **2**,637 (1959).
[18] A.J. Moerdijk, B.J. Verhaar, and A. Axelsson, Phys. Rev. A **51**, 4852 (1995).
[19] F. Pereira Dos Santos *et al.*, Phys. Rev. Lett. **89**, 233004 (2002).
[20] E. Rasel *et al.*, Eur. Phys. J. D **7**, 311-316 (1999).
[21] G. Santarelli *et al.*, Phys. Rev. Lett. **82**, 4619 (1999)
[22] F. Shimizu *et al.*, Chem. Phys. **145**, 327 (1990).
[23] Y. Sortais *et al.*, Phys. Rev. Lett. **85**, 3117 (2000).
[24] E. Tiesinga *et al.*, Phys. Rev. A **47**, 4114 (1993).
[25] P. wolf *et al.*, Phys. Rev. Lett. **90**, 060402 (2003).
[26] R.Wynands and S. Weyers, Atomic fountain clocks, Metrologia **42** S64S79, (2005)

$$\text{Ratio} = A^{(50)}_{(4-5)} / A^{(100)}_{(4-5)}$$

Ratio = 0.5006